



LUND UNIVERSITY

On the Relationship of Biogenic Primary and Secondary Organic Aerosol Tracer Compounds on the Aethalometer Model Parameters

Martinsson, Johan; Sporre, Moa; Pédehontaa-Hiaa, Guillaume; Abdul Azeem, Hafiz

Published in:
Aerosol and Air Quality Research

DOI:
[10.4209/aaqr.2020.01.0035](https://doi.org/10.4209/aaqr.2020.01.0035)

2020

Document Version:
Publisher's PDF, also known as Version of record

[Link to publication](#)

Citation for published version (APA):
Martinsson, J., Sporre, M., Pédehontaa-Hiaa, G., & Abdul Azeem, H. (2020). On the Relationship of Biogenic Primary and Secondary Organic Aerosol Tracer Compounds on the Aethalometer Model Parameters. *Aerosol and Air Quality Research*, 20(12), 2654-2668. <https://doi.org/10.4209/aaqr.2020.01.0035>

Total number of authors:
4

Creative Commons License:
CC BY

General rights

Unless other specific re-use rights are stated the following general rights apply:
Copyright and moral rights for the publications made accessible in the public portal are retained by the authors and/or other copyright owners and it is a condition of accessing publications that users recognise and abide by the legal requirements associated with these rights.

- Users may download and print one copy of any publication from the public portal for the purpose of private study or research.
- You may not further distribute the material or use it for any profit-making activity or commercial gain
- You may freely distribute the URL identifying the publication in the public portal

Read more about Creative commons licenses: <https://creativecommons.org/licenses/>

Take down policy

If you believe that this document breaches copyright please contact us providing details, and we will remove access to the work immediately and investigate your claim.

LUND UNIVERSITY

PO Box 117
221 00 Lund
+46 46-222 00 00



On the Relationship of Biogenic Primary and Secondary Organic Aerosol Tracer Compounds on the Aethalometer Model Parameters

Johan Martinsson^{1*}, Moa K. Sporre², Guillaume Pédehontaa-Hiaa¹, Hafiz Abdul Azeem³

¹ Medical Radiation Physics, Department of Translational Medicine, Lund University, Box 118, SE-22100, Malmö, Sweden

² Division of Nuclear Physics, Lund University, Box 118, SE-22100, Lund Sweden

³ Centre for Analysis and Synthesis, Department of Chemistry, Lund University, Box 118, SE-22100, Lund, Sweden

ABSTRACT

The aethalometer model has shown to offer a fast, inexpensive and robust method for source apportionment. The method relies on aerosol light absorption attribution, mass balance of the total carbon and results in a fraction of unaccounted, residual carbon that has been associated to biogenic carbon due to its presumably non-light absorbing properties. This residual carbon and its relation to tracers of biogenic primary and secondary organic aerosol was investigated at a rural measurement station in Sweden. Special focus is devoted to 3-methyl-1,2,3-butanetricarboxylic acid (MBTCA), a second-generation oxidation compound in biogenic secondary organic aerosols. The results show that the residual carbon and the biogenic tracers show a high degree of correlation and that the tracers were highly seasonally dependent with largest carbon contributions during summer. MBTCA showed positive correlation with the aethalometer model derived absorption coefficients from fossil fuel carbonaceous aerosol, stressing the suspicion that biogenic aerosol might be falsely apportioned to fossil fuel carbon in the aethalometer model. MBTCA showed an increasing degree of correlation with higher aethalometer absorption coefficient wavelengths. However, spectrophotometric analysis revealed that the ambient concentrations of MBTCA are most likely too low to give a significant response in the aethalometer. These results support the application of MBTCA as a molecular tracer for biogenic secondary organic aerosol and indicates that a large fraction of the aethalometer model residual carbon is of biogenic origin. Future studies should investigate the light absorbing properties of precursor monoterpenes such as α -pinene, their oxidation products and eventual influence on the aethalometer model.

Keywords: Aethalometer; Source apportionment; Biogenic aerosol.

INTRODUCTION

The carbonaceous aerosol contributes to approximately 20–50% to the total aerosol mass in Europe (Kanakidou *et al.*, 2005; Putaud *et al.*, 2010; Fuzzi *et al.*, 2015). Its high abundance, detrimental health effects and climate impact makes the carbonaceous aerosol crucial to study as an environmental stressor. The ambient carbonaceous aerosol mainly originates from three distinguished sources: fossil fuel combustion, biomass burning and biogenic emissions (Liousse *et al.*, 1996). Due to the detrimental effects of combustion generated aerosol particles, fossil fuel combustion and biomass burning aerosol physicochemical properties and related source apportionment have gained large attention in the past (Barregard *et al.*, 2006; Naeher *et al.*, 2007; Bolling *et al.*, 2009; Sehlstedt *et al.*, 2010; Janssen *et al.*, 2011;

Bond *et al.*, 2013). However, there are only a few source apportionment studies focusing on the biogenic carbonaceous aerosol fraction (Yttri *et al.*, 2011).

Biogenic aerosols are comprised of biogenic primary organic aerosols (BPOA) and biogenic secondary organic aerosols (BSOA). BPOA can be found as pollen, bacteria, fungal spores and plant debris. BSOA is the product of biogenic volatile organic compound (BVOC) oxidation in the atmosphere. BVOCs are used as a communicative tool as well as to handle abiotic and biotic stress and is emitted globally in large quantities from terrestrial and aquatic plants (Gabric *et al.*, 2001; Penuelas and Llusia, 2003; Sharkey *et al.*, 2008; Monson *et al.*, 2013; Glasius and Goldstein, 2016; Steinke *et al.*, 2018). Emissions of BPOA and BVOCs have been shown to increase with increasing photosynthetically active radiation (PAR) and temperature (Guenther *et al.*, 1993; Guenther *et al.*, 1995; Hakola *et al.*, 2003), which explains the dominance of the biogenic mass fraction in carbonaceous aerosol during summer (Gelencser *et al.*, 2007; Genberg *et al.*, 2011; Yttri *et al.*, 2011; Martinsson *et al.*, 2017a, b). The main BVOC is isoprene, which is emitted

* Corresponding author.

E-mail address: johan.martinsson@med.lu.se

mostly from deciduous forests with an annual emission rate of 400–600 Tg y⁻¹ (Laothawornkitkul *et al.*, 2009). Coniferous forest emits large quantities (30–500 Tg y⁻¹) of monoterpenes such as α -pinene, β -pinene, Δ^3 -carene and limonene (Räisänen *et al.*, 2008; Laothawornkitkul *et al.*, 2009; Hakola *et al.*, 2012). The α -pinene contributes to approximately 40% of the global monoterpene emissions (Guenther *et al.*, 2012). Landmasses at northern latitudes are largely covered by coniferous forests. Global climate modeling has shown that these areas are the most susceptible for global warming in terms of temperature increment (IPCC, 2013). Hence, following an increase in temperature may cause a significant increase in monoterpene emission at these latitudes (Sporre *et al.*, 2019). Consequently, global BSOA production may increase due to increased BVOC emissions.

Andersson-Sköld and Simpson (2001) showed that monoterpene BSOA may contribute to 50% of the total organic aerosol mass over the Nordic countries with α -pinene being the dominant precursor compound. Atmospheric oxidation of α -pinene can result in the production of first-generation oxidation products including pinic acid, pinonic acid and pinonaldehyde (Larsen *et al.*, 2001; Jaoui and Kamens, 2002; Lee *et al.*, 2006). The 3-methyl-1,2,3-butanetricarboxylic acid (MBTCA) is produced by gas-phase oxidation of pinonic acid (Muller *et al.*, 2012), and is thus a second-generation oxidation product from α -pinene. MBTCA has been suggested and used as a tracer for BSOA originating from OH-initiated oxidation of monoterpene emissions (Szmigielski *et al.*, 2007; Zhang *et al.*, 2010). MBTCA has low volatility ($1.8 \pm 1.3 \cdot 10^{-3}$ $\mu\text{g m}^{-3}$) and an atmospheric lifetime of 3–5 days assuming an daily average OH radical concentration of 10^6 molecules cm⁻³ (Donahue *et al.*, 2013; Kostenidou *et al.*, 2018), and has been detected and measured in various terrestrial locations on Earth (Kubatova *et al.*, 2000; Kubatova *et al.*, 2002; Gao *et al.*, 2006; Lewandowski *et al.*, 2007; Kourtchev *et al.*, 2008a, b; Fu *et al.*, 2009; Kourtchev *et al.*, 2009; Yasmeen *et al.*, 2011; Vogel *et al.*, 2013; Martinsson *et al.*, 2017c). Recently, Kostenidou *et al.* (2018) presented a high-resolution aerosol mass spectrometry (HR-AMS) spectra of MBTCA and suggested to use the *m/z* 141 as a signature for MBTCA in AMS measurements. Hence, MBTCA has great potential acting as a high time resolution tracer for BSOA emissions.

Source apportionment as a concept offers a basis for decision making in order to mitigate health and climate effects of carbonaceous aerosol. Low cost, low maintenance and high time resolution are desirable attributes of an auspicious source apportionment method. The aethalometer model, originally presented by Sandradewi *et al.* (2008a), utilizes differences in the spectral light absorption of fossil fuel combustion and wood burning aerosol to apportion the organic aerosol mass to these two sources. All non-light absorbing carbon present are, through mass balance of the total carbon apportioned as residual carbon, which is thought to contain large portions of the biogenic carbon as BSOA or BPOA. The aethalometer model has been proven to deliver a robust source apportionment with high time resolution to a low cost (Martinsson *et al.*, 2017b). In a recent study by Martinsson *et al.* (2017b) it was shown that the wood burning

parameter from the aethalometer model correlated satisfactory with the chemical tracer for wood burning, levoglucosan. This result can be viewed as a strong indicator of the method working correctly for wood burning apportionment. Hence, the aethalometer model combustion components, wood burning and fossil fuel combustion, has been evaluated against strong source indicators, tracers, such as levoglucosan and radiocarbon (¹⁴C). BSOA compounds have been shown to have low or negligible light absorption due to absence of conjugated molecular systems (Nakayama *et al.*, 2010; Henry and Donahue, 2012; Laskin *et al.*, 2014). However, whether increased mass concentrations of non-light absorbing carbon have effect on filter based light absorption techniques for source apportionment purposes remains unexplored. In this study we want to investigate the aethalometer model and the presumably non-light absorbing residual carbon and its possible strong association to biogenic carbon through measurement of a biogenic tracers and in particular a tracer for monoterpene oxidation, MBTCA.

METHODS

Measurement Site and Sampling

Ambient aerosol sampling was conducted at the aerosol, clouds and trace gases research infrastructure (ACTRIS) and European Monitoring and Evaluation Programme (EMEP) Vavihill measurement station. Vavihill measurement station was located on a ridge at an altitude of 172 m.a.s.l. (56°01'N, 13°09'E) in southern Sweden. The surrounding landscape consists of mixed deciduous and coniferous forests. The measurement station itself was in the middle of a small pasture that is occasionally visited by grazing cattle from May to September. The cities closest to Vavihill are Helsingborg, Malmö and Copenhagen located at distances of 20, 50 and 65 km, respectively, in the west, south-west direction. Aerosols were sampled through a PM₁₀ inlet at 38 L min⁻¹ on pre-heated (900°C for four hours) 47 mm quartz fiber filters (Pallflex 2500QAT-UP) during 72 h using an automatic low volume sampler (Leckel SEQ46/50). Active carbon denuders were installed in the sampling line together with double filters in order to correct for sampling artifacts caused by VOCs, the denuders were replaced once every year. Following sampling, the filters were placed in petri dishes, wrapped in aluminum foil and stored in a -18°C freezer until analysis. Sampling was conducted continuously from 2007 until 2017. In this paper we used filters that were sampled during April 2013 to August 2013 (N = 47) and September 2015 to March 2016 (N = 61). The reason for two incoherent sampling periods was the purpose to cover all months in a year together with varying instrument availability and functioning during the operation of the measurement station. The Vavihill measurement station was decommissioned during 2018 and all measurement activity has been moved to the ACTRIS, EMEP and Integrated Carbon Observation System in Sweden (ICOS), Hyltemossa measurement station 20 km east of Vavihill.

Thermo-optical Analysis

Organic carbon (OC), elemental carbon (EC) and total

carbon (TC) was derived from thermo-optical analysis of the filters using a DRI carbon analyzer (model 2001) with the EUSAAR_2 analytic protocol (Cavalli *et al.*, 2010). The method utilizes the refractive properties of the carbonaceous aerosol to evolve and quantify the carbon at different temperatures in different atmospheres. In short, the EUSAAR_2 protocol initiate the analysis by allowing OC from a 0.5 cm² filter to evolve in an inert He-atmosphere to a maximum temperature of 570°C. During the heating process a 633 nm He/Ne laser is continuously irradiating the filter, a photodetector is mounted 180° from the laser light path to measure the light transmission through the filter. When the laser transmission signal reaches its baseline value the remaining carbon is defined to be EC. The EC is then heated from 500 to 850°C in a 2% O₂ atmosphere, allowing refractory carbon to be combusted. All carbon that are evolved from the filter are oxidized to CO₂. The CO₂ is further reduced to methane by passing hydrogen gas over a zinc catalyst. Finally, the methane is quantified using a flame ionization detector (FID). A recent study by Cavalli *et al.* (2016) estimated the thermo-optical analysis uncertainty of TC from Vavihill filter samples to 17% relative standard deviations (RSD).

Light Absorption Measurements

The light absorption of ambient aerosols was measured with an aethalometer (AE33, Magee Scientific). Aerosols were sampled with a flow of 5 L min⁻¹ through a PM₁₀ inlet to the aethalometer where the aerosol were deposited on a filter spot. The aethalometer filter spot is continuously irradiated by seven LEDs with wavelengths from 370 nm to 950 nm. The light attenuation was measured with photodetectors with a time resolution of 1 min. The aethalometer, model AE33, was developed to correct for the artefacts common in filter-based light absorption techniques, the shadowing effect and the filter matrix scattering effect (Drinovec *et al.*, 2015). These artefacts are described in detailed by Weingartner *et al.* (2003).

The aethalometer output parameter is attenuation coefficients which, after automatic artefact corrections, are transformed to absorption coefficients for each wavelength, $b_{abs}(\lambda)$, with the unit of m⁻¹. Further, the $b_{abs}(\lambda)$ can be converted to mass concentration of BC (μg m⁻³) by division of the specific mass absorption coefficients ($\sigma_{abs}(\lambda)$, MAC), with the unit m² g⁻¹.

The Aethalometer Model

For the source apportionment of carbon mass the aethalometer model originally presented by Sandradewi *et al.* (2008a) with modifications by Martinsson *et al.* (2017b) was used. In the aethalometer model the total aerosol light absorption are attributed to light absorbing carbon from fossil fuel combustion (FF) or wood burning (WB) according to Eqs. (1)–(3):

$$b_{abs}(\lambda) = b_{absFF}(\lambda) + b_{absWB}(\lambda) \quad (1)$$

$$\frac{b_{absFF}(370 \text{ nm})}{b_{absFF}(950 \text{ nm})} = \left(\frac{370}{950} \right)^{-AAE_{FF}} \quad (2)$$

$$\frac{b_{absWB}(370 \text{ nm})}{b_{absWB}(950 \text{ nm})} = \left(\frac{370}{950} \right)^{-AAE_{WB}} \quad (3)$$

In these equations, the AAE is the absorption Ångström exponent that describes the spectral absorption dependence of the source specific aerosols. These parameters need to be accurately pre-defined and this is commonly achieved by using reference values from laboratory or field experiments. In this study we used $AAE_{WB} = 1.81$ and $AAE_{FF} = 1.0$, values that were used and motivated in the study by Martinsson *et al.* (2017b). From the derived aethalometer model absorption coefficients, b_{absFF} and b_{absWB} , it is now possible to calculate the source apportioned carbonaceous aerosol mass (CM). CM is thought to consist of three components, where CM_{FF} and CM_{WB} are the source apportioned carbon mass concentrations, and CM_{Bio} is a residual non-light absorbing component:

$$TC = CM_{FF} + CM_{WB} + CM_{Bio} = C_1 \cdot b_{absFF}(950 \text{ nm}) + C_2 \cdot b_{absWB}(370 \text{ nm}) + CM_{Bio} \quad (4)$$

In this study we want to compare the residual carbon, CM_{Bio} , to biogenic aerosol tracer compounds. Hence, solving Eq. (4) as a multilinear regression, leaving CM_{Bio} as a fixed intercept as originally proposed by Sandradewi *et al.* (2008a) is not convenient when aiming to study potential variation in CM_{Bio} . Hence, we use the alternative solution where CM_{Bio} is allowed to vary outside the Eqs. (5)–(6) that are used to calculate C_1 and C_2 .

$$\frac{TC}{b_{absWB}(370 \text{ nm})} = C_1 \frac{b_{absFF}(950 \text{ nm})}{b_{absWB}(370 \text{ nm})} + C_2 + \frac{CM_{Bio}}{b_{absWB}(370 \text{ nm})} \quad (5)$$

$$\frac{TC}{b_{absFF}(950 \text{ nm})} = C_2 \frac{b_{absWB}(370 \text{ nm})}{b_{absFF}(950 \text{ nm})} + C_1 + \frac{CM_{Bio}}{b_{absFF}(950 \text{ nm})} \quad (6)$$

C_1 and C_2 can be calculated as the slope of the linear regression of Eqs. (5)–(6) as in Martinsson *et al.* (2017b). The calculations for deriving C_1 and C_2 are made exclusively for samples collected during winter (December–February), in this way the presumed non-light absorbing biogenic carbon (CM_{Bio}) are minimized as a factor of interference. As opposed to Sandradewi *et al.* (2008), CM_{Bio} is here allowed to vary outside the linear regressions:

$$CM_{Bio} = TC - CM_{FF} - CM_{WB} \quad (7)$$

The linear slopes representing C_1 and C_2 was estimated to 446 853 and 96 272 μg m⁻², respectively, based on 30 data points obtained during the winter (December–February). The coefficient of determination, R^2 , was 0.39 for the C_1 parameter and 0.31 for the C_2 parameter, these numbers are in similar range to the parameter statistics found in Martinsson *et al.* (2017b). Further, since CM_{Bio} is expected to be suppressed during winter, the last division term in Eqs. (5)–(6) should result in a small number relative to the estimated C parameters.

Hence, the intercept of the linear fit of Eq. (5) (i.e., $C_2 + CM_{Bio}/b_{absWB}(370nm)$) should be very close to the estimated C_2 parameter through the linear fit of Eq. (6). The same concept is applicable for quality control of the C_1 parameter. The intercept of the linear regression of Eq. (5) was estimated to 82 571 which is deviating by 14% to the estimated C_2 parameter. The intercept of the linear regression of Eq. (6) was estimated to 396 936 which is deviating by 11% to the estimated C_1 parameter. These deviations are smaller than the ones estimated in Martinsson *et al.* (2017b) who found deviations of 22 and 15% of the C_1 and C_2 parameters to their intercepts, respectively. The linear regressions plots are displayed in Figs. S1 and S2 in the supplement.

As mentioned earlier it is also possible to solve Eq. (4) as a multilinear regression as originally proposed by Sandradewi *et al.* (2008a). However, in such case the CM_{Bio} would be fixed as a residual as a constant and not be allowed to vary in time. Further, this was examined in Martinsson *et al.* (2017b) and gave unrealistic high C_1 parameter. Hence, for the purpose of this study the originally proposed solution to Eq. (4) will not be considered here.

Analysis of Biogenic Aerosol Tracers

Analysis of six emission markers including levoglucosan, arabinol, fructose, sucrose, cis-pinonic acid and 3-methyl-1,2,3-butane tricarboxylic acid was performed according to the method of Pietrogrande *et al.* (2014). Briefly, filter punches were divided into small pieces using a sterile surgical blade. Extractions were performed in ultrasonic bath for 15 min using 10 mL of methanol and dichloromethane mixture (9:1). Extracts were filtered prior to analysis using a 25 mm (pore size 0.45 μm) polypropylene syringe filter.

Extracts were analyzed by supercritical fluid chromatography (SFC, Agilent 1260 Infinity II) coupled to Triple Quadrupole Mass Spectrometer (Agilent 6460 system) using the following conditions. Initially a mobile phase (CO_2 /methanol) with composition of 93:7% was used for 5 min followed by a composition of 80:20% for 6.5 min and returning back to 93:7% at 7.5 minutes. Mobile phase and make-up (methanol) flow rates were maintained at 2.5 mL and 0.5 mL, respectively. Injection volume of 2 μL was used for all samples while column temperature was maintained at 50°C. The back-pressure regulator was programmed for 135 bars and 50°C throughout the analysis. Mass spectrometric analysis was performed using gas temperature of 80°C, gas flow of 20 L min^{-1} and nebulizer pressure of 30 psi. Sheath gas temperature and flow were 250°C and 12 L min^{-1} , respectively. Capillary and nozzle voltages were set to 3000 V and 1000 V, respectively, whereas an electron multiplier voltage of 400 V was used. Identification and quantification of emission markers was performed using retention times and SIM using m/z 161, 151, 179, 341, 183, 203 for levoglucosan, arabinol, fructose, sucrose, cis-pinonic acid and 3-methyl-1,2,3-butane tricarboxylic acid, respectively.

Spectrophotometric Analysis

A standard of 3-methyl-1,2,3-butane tricarboxylic acid (MBTCA) was purchased from Toronto Research Chemicals Inc., Toronto, Canada. Five 25 mL solutions of 10, 20, 100,

250 and 500 mmol L^{-1} was produced by dissolving weighed MBTCA powder in ultrapure water (MilliQ). Spectrophotometric analyses were carried out using a portable spectrophotometer (USB-650, Red Tide Spectrometer, OceanOptics) using a wavelength range of 200–850 nm. 2 mL of ultrapure water was placed in a quartz cuvette and used as background measurement. The cuvette was then rinsed with ultrapure water before adding any MBTCA solution. Output data from the spectrophotometer was absorbance (A). Absorbance was then transformed to absorption per density ($\alpha \rho^{-1}$) according to Chen and Bond (2010):

$$\alpha \rho^{-1} = \frac{A}{c \cdot L} \cdot \ln(10) \quad (8)$$

L is the optical path length, which in this case was 1 cm and c is the concentration of the MBTCA solutions expressed as mass per volume.

Trajectory Analysis

The Hybrid Single Particle Lagrangian Integrated Trajectory Model (HYSPLIT) (Draxier and Hess, 1998; Stein *et al.*, 2015) was used to study the history of the air mass carrying the particles sampled on the filters and measured by the aethalometer. Gridded meteorological data from the Centre of Environmental Predictions (NCEP) Global Data Assimilation System (GDAS) were used as input to trajectory model. Back-trajectories were calculated at an hourly frequency 120 h backward in time and the trajectories started 100 m above ground at the Vavihill measurement site. For each filter sample, 72 trajectories were used since the sampling time was 72 h. Four regions of origin were defined (Northeast = 0–90°; Southeast = 90–180°; Southwest = 180–270°; Northwest = 270–360°) and for each sample the fraction of time that the air-mass spent over each of the regions of origin was calculated.

Meteorological Observations

Temperature and precipitation data were obtained through the website of the Swedish Meteorological and Hydrological Institute (SMHI). The closest observation points for temperature and precipitation to the Vavihill measurement station was found in the city of Helsingborg (56°03'N, 12°77'E) and Gillastig (56°01'N, 13°23'E), respectively. Helsingborg is located 20 km west of Vavihill while Gillastig is located 3 km southeast of Vavihill.

RESULTS AND DISCUSSION

Temporal Variation of Measured Parameters

Fig. 1(a) shows the temporal variations of OC and EC for the measurement period. Spring and summer showed similar concentrations levels for OC ($OC_{meanSpring} = 1.17 \mu g m^{-3}$; $OC_{meanSummer} = 1.28 \mu g m^{-3}$) and EC ($EC_{meanSpring} = 0.20 \mu g m^{-3}$; $EC_{meanSummer} = 0.15 \mu g m^{-3}$). Both OC and EC were elevated in the autumn ($OC_{mean} = 1.68 \mu g m^{-3}$; $EC_{meanAutumn} = 0.38 \mu g m^{-3}$) which is mainly caused by the two peaks during 2015-10-18 and 2015-11-02, these two periods had slightly lower temperature (7.9 and 8.8°C) than the average temperature of

the whole autumn ($T_{\text{meanAutumn}} = 9.3^{\circ}\text{C}$). Hence, it can be expected that the higher carbonaceous aerosol concentrations during these periods was caused by and increased activity of residential wood burning. As expected, the levoglucosan concentrations was also elevated during these periods (0.35 and $0.25 \mu\text{g m}^{-3}$ compared to the autumn mean of $0.08 \mu\text{g m}^{-3}$). Winter data display $\text{OC}_{\text{meanWinter}}$ and $\text{EC}_{\text{meanWinter}}$ of 0.96 and $0.21 \mu\text{g m}^{-3}$, respectively. As observed during the autumn, suppressed temperature during 2016-01-04 and 2016-01-13 (-3.2 and 0.0°C ; $T_{\text{meanWinter}} = 2.3^{\circ}\text{C}$) resulted in two distinct peaks in OC and EC and was associated with increased levoglucosan concentrations (0.15 and $0.15 \mu\text{g m}^{-3}$ compared to winter mean of $0.10 \mu\text{g m}^{-3}$) and also increased AAE

(1.58 and 1.52 compared to winter mean of 1.39 , Fig. 1(b)). The transition from the 2013 to the 2015–2016 measurement period did not result in any abrupt and significant change in the carbonaceous aerosol concentration.

The absorption Ångström exponent (AAE) experience low levels during the spring and summer of 2013 and rapidly increases with the transition to the 2015 and 2016 measurement period. The increase from summer to autumn and winter is expected due to increased wood burning as the temperature decreases, however this rapid shift in AAE could be worth investigating more in depth. This transition is actually followed by a rather steep decrease in ambient temperature, from a quite stable summer temperature during

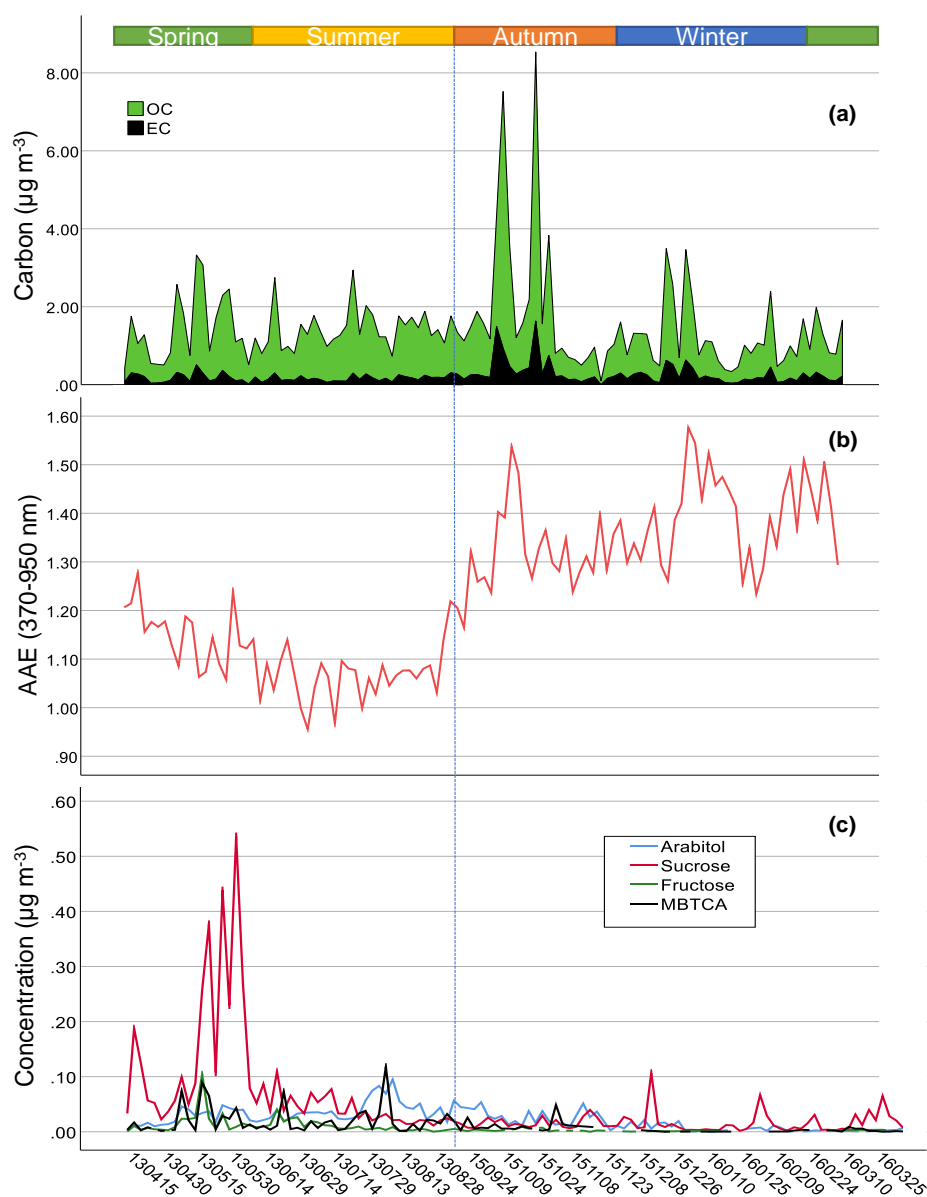


Fig. 1. (a) OC and EC during the measurement period. The dotted line in the transition between summer and autumn displays the junction between the measurement period of 2013 and 2015–2016. $N = 111$. (b) Temporal variation of the absorption Ångström exponent (AAE) during the measurement period. The AAE was calculated by a linear fit using absorption coefficient in all seven available wavelengths (370–950 nm). $N = 106$. (c) Temporal variation of the measured biogenic tracer compounds. $N_{\text{Arabitol}} = 103$; $N_{\text{Sucrose}} = 115$; $N_{\text{Fructose}} = 72$; $N_{\text{MBTCA}} = 81$.

2013 with a mean and standard deviation of $16.9 \pm 2.1^\circ\text{C}$ to around 7°C within a month (i.e., from 2015-09-12 to 2015-10-12), presumably leading to a rapid increase in residential wood combustion. During this month of rapidly increasing AAE we can also see a fivefold increase in levoglucosan concentrations (i.e., from 0.01 to $0.05\ \mu\text{g m}^{-3}$). Hence, the steep increase in AAE during the transition between measurement periods can be explained by decreasing temperatures and increased wood burning rather than any operational changes within the aethalometer instrument. The overall trend is although clear with low values during the cold season and the opposite during summer. AAE and temperature display a strong relationship ($R^2 = 0.76$). The seasonal AAE values is comparable to the levels found in Martinsson *et al.* (2017b).

Temporal variations of measured biogenic tracers are displayed in Fig. 1(c) and in Table 1. The concentrations of all tracers are, as expected, elevated during summer and suppressed during winter. MBTCA was during spring and summer on similar concentration levels to what has been found in previous European studies (Kourtchev *et al.*, 2009; Kristensen and Glasius, 2011; Maenhaut *et al.*, 2017; Martinsson *et al.*, 2017c). Elevated MBTCA concentrations was further associated to raising temperatures ($R^2 = 0.23$, $p < 0.01$), an effect that was peculiarly prominent during spring ($R^2 = 0.56$, $p < 0.01$) and summer ($R^2 = 0.27$, $p < 0.01$). MBTCA showed a positive, although weak, whole-year correlation to air masses from southeast ($R^2 = 0.09$, $p = 0.03$). The correlation was stronger during spring and summer ($R^2 = 0.20$, $p = 0.04$; $R^2 = 0.35$, $p < 0.01$). The remaining air mass directions (NW, NE and SW) had a negative impact on the MBTCA concentration, this was particularly pronounced for air masses arriving from the northwestern sector ($R^2 = 0.08$, $p < 0.01$), a sector dominated by the North Sea and Atlantic Ocean. Arabitol, a tracer of fungal spores, hence primary biogenic organic aerosol (Bauer *et al.*, 2008), was in a comparable concentration range ($\text{Arabitol}_{\text{meanSummer}} =$

$39.5\ \text{ng m}^{-3}$) as found in Yttri *et al.* (2011) who measured biogenic tracers at four Scandinavian measurement stations during summer, Vavihill included. As MBTCA, arabitol also showed a strong positive temperature dependence ($R^2 = 0.54$), with a maximum concentration around $18\text{--}21^\circ\text{C}$ which is a pattern that also have been observed by others (Burshtein *et al.*, 2011). Arabitol showed no trends of variability with different air mass origins. Sucrose is a tracer of mainly pollen, but also soil biota and lichens (Caseiro *et al.*, 2007; Yttri *et al.*, 2007), and were highest during spring and summer. Pollen emissions by plants usually peaks in the beginning of the annual vegetation cycle (Siljamo *et al.*, 2008; Yli-Panula *et al.*, 2009; Manninen *et al.*, 2014) which may be the explanation for finding the seasonal maximum of sucrose during spring, a phenomenon already observed by Yttri *et al.* (2007). Fructose found in aerosol can originate from the fruits of terrestrial plants but is also a tracer of pollen and vascular plant debris (Cowie and Hedges, 1984; Speranza *et al.*, 1997). The fructose concentration followed similar temporal pattern as sucrose but was a factor 5–15 lower, similar observations has been made by others (Yttri *et al.*, 2007; Verma *et al.*, 2018). Both sucrose and fructose showed weak relationships to temperature ($R^2 = 0.11$, for both), although analyzing the seasonal temperature correlation displayed stronger relationship during spring ($R^2 = 0.55$ for sucrose; $R^2 = 0.60$ for fructose) underlining the importance of the springtime pollen bursts. Further, both sugars showed no correlation with any air mass origin.

Source Apportionment by the Aethalometer Model

The temporal behavior of the aethalometer model output parameters is showed in Fig. 2(a). The carbon concentration reflects the carbonaceous content, as displayed in Fig. 1(a), while the distribution between the sources reflects the AAE and the aethalometer model. CM_{FF} show low variation in mass concentration throughout the year (mean = $0.86 \pm$

Table 1. Seasonal means and standard deviations of the main measured and calculated parameters as well as meteorological data on temperature and precipitation.

	Winter	Spring	Summer	Autumn
TC ($\mu\text{g m}^{-3}$)	1.17 ± 0.87	1.36 ± 0.80	1.42 ± 0.56	2.06 ± 2.00
OC ($\mu\text{g m}^{-3}$)	0.96 ± 0.70	1.17 ± 0.70	1.28 ± 0.50	1.68 ± 1.66
EC ($\mu\text{g m}^{-3}$)	0.21 ± 0.17	0.20 ± 0.12	0.15 ± 0.07	0.38 ± 0.39
AAE	1.39 ± 0.09	1.20 ± 0.12	1.07 ± 0.06	1.31 ± 0.09
Levoglucosan (ng m^{-3})	104.76 ± 58.66	55.65 ± 36.65	13.19 ± 7.07	77.22 ± 78.41
MBTCA (ng m^{-3})	1.03 ± 1.31	14.95 ± 24.58	19.00 ± 23.84	12.58 ± 12.07
Arabitol (ng m^{-3})	7.77 ± 6.96	16.49 ± 16.15	39.52 ± 19.27	27.17 ± 15.05
Sucrose (ng m^{-3})	15.84 ± 21.90	84.90 ± 111.28	65.52 ± 99.34	16.29 ± 8.61
Fructose (ng m^{-3})	0.88 ± 0.35	16.06 ± 24.14	10.22 ± 8.55	3.29 ± 2.28
cis-Pinonic acid	2.86 ± 0.96	4.18 ± 3.28	5.67 ± 7.87	3.52 ± 2.64
CM_{FF} ($\mu\text{g m}^{-3}$)	0.68 ± 0.42	0.97 ± 0.57	0.81 ± 0.31	1.02 ± 0.85
CM_{WB} ($\mu\text{g m}^{-3}$)	0.64 ± 0.73	0.23 ± 0.21	0.05 ± 0.05	0.62 ± 0.76
CM_{Bio} ($\mu\text{g m}^{-3}$)	-0.14 ± 0.55	0.17 ± 0.81	0.56 ± 0.46	0.43 ± 0.92
$\text{CM}_{\text{FF(Mod)}}$ ($\mu\text{g m}^{-3}$)	0.25 ± 0.15	0.36 ± 0.21	0.30 ± 0.11	0.38 ± 0.31
$\text{CM}_{\text{WB(Mod)}}$ ($\mu\text{g m}^{-3}$)	0.70 ± 0.80	0.26 ± 0.23	0.05 ± 0.06	0.66 ± 0.83
$\text{CM}_{\text{Bio(Mod)}}$ ($\mu\text{g m}^{-3}$)	0.22 ± 0.47	0.76 ± 0.85	1.08 ± 0.50	1.03 ± 1.09
Temperature ($^\circ\text{C}$)	2.28 ± 4.32	7.98 ± 4.93	16.89 ± 2.07	9.27 ± 3.49
Precipitation (mm)	3.28 ± 3.33	1.19 ± 1.64	1.88 ± 2.69	3.03 ± 3.60

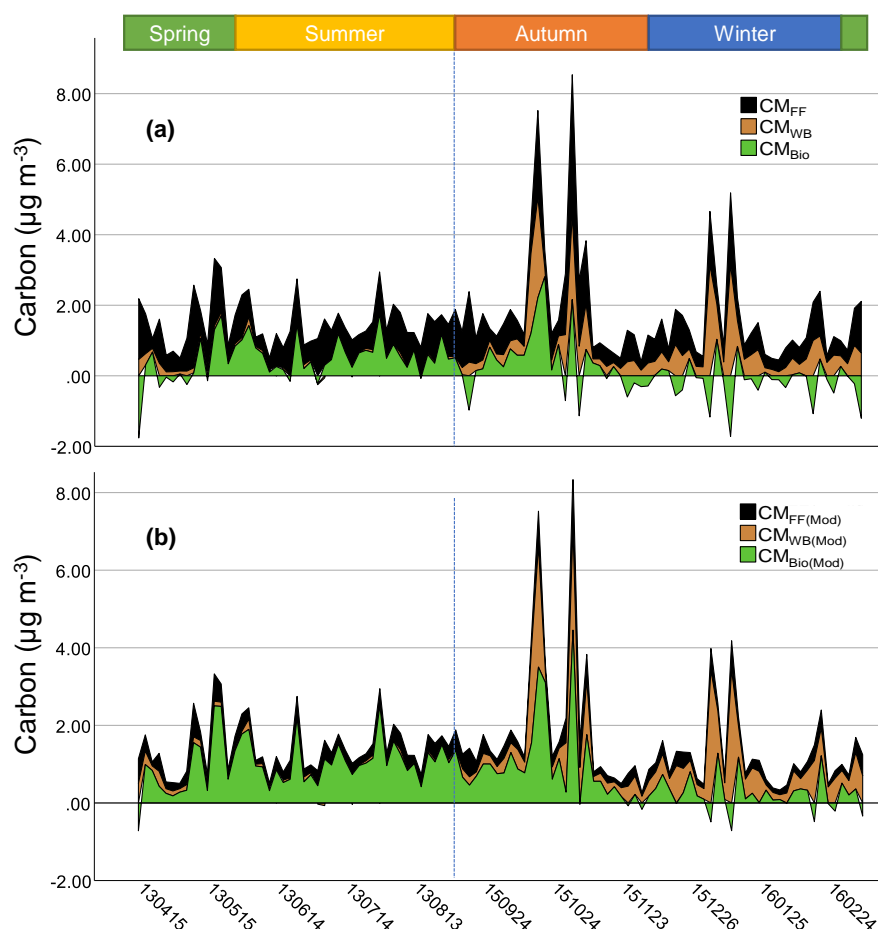


Fig. 2. (a) The originally calculated CM-parameters using the aethalometer model ($C_1 = 446\,853\ \mu\text{g m}^{-2}$; $C_2 = 96\,272\ \mu\text{g m}^{-2}$). (b) Modified and optimized CM-parameters ($C_1 = 164\,974\ \mu\text{g m}^{-2}$; $C_2 = 105\,076\ \mu\text{g m}^{-2}$). The dotted line in the transition between summer and autumn displays the transition between the measurement period of 2013 and 2015–2016. $N = 106$.

$0.57\ \mu\text{g m}^{-3}$), contributing in average with 68% to the TC mass concentration. This is a factor 2.4 higher than the contribution to TC found at Vavihill in Martinsson *et al.* (2017b) (mean contribution = 28%) and could be an indicator of an erroneous C_1 parameter. CM_{WB} show a distinct seasonal pattern with elevated concentrations during winter (mean = $0.64 \pm 0.73\ \mu\text{g m}^{-3}$) compared to summer (mean = $0.05 \pm 0.05\ \mu\text{g m}^{-3}$). The CM_{WB} contribution to TC was maximized during winter with 55%, this number is in line with previous findings from Vavihill (Martinsson *et al.*, 2017b). CM_{Bio} peaked during summer with a mean mass concentration of $0.57 \pm 0.46\ \mu\text{g m}^{-3}$, leading to a TC contribution of 35%. The carbon contribution of CM_{Bio} to TC is here a factor two lower than the value found in Martinsson *et al.* (2017b). Due to the aethalometer model setup in Eq. (7) it is possible for CM_{Bio} to adopt negative values if the sum of CM_{FF} and CM_{WB} exceeds TC. Negative values of CM_{Bio} was frequently observed during winter, thus leading to a winter average mass concentration of $-0.14 \pm 0.55\ \mu\text{g m}^{-3}$. It can be feasible to allow some exceedances by the sum of CM_{FF} and CM_{WB} to the TC concentration, leading to negative CM_{Bio} values. However, with the current estimated C-parameters there are cases where CM_{FF} and CM_{WB} are in the range of 2–4 times higher than TC, which obstruct any endeavor to accomplish

a sound source apportionment. It is indeed a non-trivial task to explain the highly elevated C_1 parameter found in this study. By studying the linear regression that was used to obtain the C_1 parameter (Fig. S1), it is evident that there are no clear outliers that could explain the elevated slope of the regression line. Hence, from a statistical point of view, it seems like the slope is correct, and that the issue is instead systematic. Another bias might occur when organic aerosol coats a soot core and hence increases the MAC value of the aerosol (Bond and Bergstrom, 2006). This means higher aerosol light absorption per unit mass. If there would be a high extent of organic coating (i.e., high MAC) during the C parameter calibration period (winter) lower C parameters would be obtained, compared to higher C parameters which would be the case if only fresh soot were detected (i.e., lower MAC). If the coating (or MAC value) during the measurement period will differ greatly from the mean MAC value during the calibration period a bias will be introduced which then might lead to over- or underestimation of either parameter (CM_{FF} , CM_{WB} or CM_{Bio}).

Sensitivity Analysis and Optimization of C_1 and C_2 Parameters

Unrealistically high C_1 parameter results in an unrealistic

apportionment of carbon to fossil sources. In this case, the C_1 parameter is that high that it generates CM_{FF} values which exceeds TC during 14 occasions. CM_{WB} contribution to TC is similar to what was found in Martinsson *et al.* (2017b), however the sum of unrealistically high CM_{FF} and realistic CM_{WB} still creates a large deficit in CM_{Bio} . Hence, the C_1 parameter, and consequently the CM_{FF} , needs to be adjusted to lower values in order to proceed with the analysis. Hence, we performed a sensitivity analysis in order to optimize the selection of C-parameters.

Averaging the C-parameters from this study with the respective values from Martinsson *et al.* (2017b) seems rational since the studies are conducted at the same measurement site, under similar circumstances and the performed measurements were conducted close in time to each other (i.e., 2013 and 2015–2016 vs. 2014–2015). Hence, combining the estimated C_1 parameter from this study with the C_1 parameter from Martinsson *et al.* (2017b) to a mean value will only decrease the C_1 parameter from $446\,853\,\mu\text{g m}^{-2}$ to $330\,660\,\mu\text{g m}^{-2}$, i.e., a decrease by 26%. Another possibility is to use the C_1 parameter found in Martinsson *et al.* (2017b), $214\,467\,\mu\text{g m}^{-2}$. This procedure would result in a decrease of the C_1 parameter by 52%. However, the validity of this value is still challenged by the results presented in Martinsson *et al.* (2017b) who found that the aethalometer model apportioned fossil fuel carbonaceous aerosol was a factor 1.3 higher than fossil fuel carbon apportioned by radiocarbon and levoglucosan. Hence, as a final step, we embrace the results from Martinsson *et al.* (2017b) and divide the C_1 parameter with a factor of 1.3 and get a final value of the C_1 parameter of $164\,974\,\mu\text{g m}^{-2}$.

Since the contribution of CM_{WB} to TC is similar to the study by Martinsson *et al.* (2017b), we will only fine-tune the C_2 parameter by using the average from the current study and from Martinsson *et al.* (2017b). The averaged C_2 parameter is $105\,076\,\mu\text{g m}^{-2}$, which is only 9% higher than the original value estimated in this study ($C_2 = 96\,272\,\mu\text{g m}^{-2}$), hence leading to small differences in the apportionment of wood burning carbonaceous aerosol.

It should be noted that using C parameters from other studies during different time periods might, even if the measurement location is constant, introduce bias into the source apportionment. However, with the more comparable results to previous conducted studies where radiocarbon and levoglucosan were used in the source apportionment it is likely that this methodology makes the source apportionment more realistic. Ideally, one should use high time resolved measurements (i.e., aerosol mass spectrometer and aethalometer measurements) during several winters in order to estimate more robust C parameters.

With the new C-parameters ($C_1 = 164\,974\,\mu\text{g m}^{-2}$; $C_2 = 105\,076\,\mu\text{g m}^{-2}$) in place it is possible to evaluate the improvement of the apportionment through comparisons and correlations with source specific tracer compounds. The modified apportionment parameters are denoted $CM_{FF(\text{Mod})}$, $CM_{WB(\text{Mod})}$ and $CM_{Bio(\text{Mod})}$. A quick comparison of the source contributions from this study to the study by Martinsson *et al.* (2017b) show a clear improvement. The $CM_{FF(\text{Mod})}$ is now contributing with 25% to TC over the measurement period which is in line with Martinsson *et al.* (2017b) who found

CM_{FF} to be in the range of 21–35%. In this range we find the $CM_{FF(\text{Mod})}$ in the lower end due to the use of the 1.3 factor as explained above. $CM_{WB(\text{Mod})}$ show agreement with the contribution levels found in Martinsson *et al.* (2017b), with low contribution during summer (4% to reference of 6%) and high contributions during winter (60% to reference of 57%). Further, $CM_{WB(\text{Mod})}$ shows a significant correlation with levoglucosan (Fig. 3, $R^2 = 0.462$, $p < 0.01$), with a slightly higher coefficient of determination compared to the original CM_{WB} ($R^2 = 0.458$). $CM_{Bio(\text{Mod})}$ shows excellent conformity in TC contribution when compared to Martinsson *et al.* (2017b) with high contribution in summer (74% to reference of 72%) and low during winter (14% to reference of 8%). The contribution during autumn (49% to reference of 49%) and spring (42% to 42%) was on a significant level, as also showed in Martinsson *et al.* (2017b). Again, higher values of $CM_{Bio(\text{Mod})}$ during summer and winter compared to the reference values obtained in Martinsson *et al.* (2017b) may depend on the 1.3 reduction factor of the C_1 parameter. CM_{Bio} displayed a rather poor correlation to MBTCA ($R^2 = 0.14$, $p < 0.01$), however this correlation was improved when comparing MBTCA to the modified apportioned biogenic carbon, $CM_{Bio(\text{Mod})}$ (Fig. 4, $R^2 = 0.27$, $p < 0.01$). The correlation was further slightly improved for arabitol ($R^2 = 0.13$ vs. $R^2 = 0.12$) and for fructose ($R^2 = 0.06$ vs. $R^2 = 0.03$), while the correlation with sucrose was unaffected ($R^2 = 0.10$ vs. $R^2 = 0.10$). Even though the correlation improved for most biogenic tracers, it still can seem low. This is because the whole-year correlation is presented which also accounts for winter data where the concentration of both the biogenic tracers and $CM_{Bio(\text{Mod})}$ is in general low, with high variability, resulting in very poor correlations ($R^2_{\text{MBTCA}} = 0.03$; $R^2_{\text{Arabitol}} = 0.10$; $R^2_{\text{Sucrose}} = 0.01$; $R^2_{\text{Fructose}} = 0.03$). Seasonal correlation analysis of the biogenic tracers and $CM_{Bio(\text{Mod})}$ show that the correlation is strong during spring for MBTCA ($R^2 = 0.70$, $p < 0.01$), arabitol ($R^2 = 0.64$, $p < 0.01$), sucrose ($R^2 = 0.56$, $p < 0.01$) and fructose ($R^2 = 0.42$, $p < 0.01$). The correlation during summer exhibit more straggling numbers where MBTCA still has a fairly high coefficient of determination to $CM_{Bio(\text{Mod})}$ ($R^2 = 0.33$, $p < 0.01$) while the three other biogenic tracers display very low coefficients ($R^2_{\text{Arabitol}} = 0.03$, $p = 0.034$; $R^2_{\text{Sucrose}} = 0.05$, $p = 0.25$; $R^2_{\text{Fructose}} = 0.05$, $p = 0.25$). It is possible that this discrepancy can be explained by continued photooxidation of α -pinene, hence MBTCA formation, during summer while the activity in pollen and fungi spore production is reduced. Manninen *et al.* (2014) analyzed pollen and other BPOA from the Hyytiälä measurement station in Finland and found that the pollen concentration peaked in May while the other BPOA (including fungal spores) peaked in August or September. This finding is consistent with the temporal concentration variation for arabitol, sucrose and fructose as displayed in Fig. 1(c) and Table 1.

MBTCA and the other measured biogenic aerosol parameters presented here do unfortunately not act as a broad biogenic activity index. With the current selected chemical compounds, it is mainly possible to get an indication of the coniferous plant activity (i.e., large emitters of α -pinene). Oxidation products from deciduous plant VOC emissions

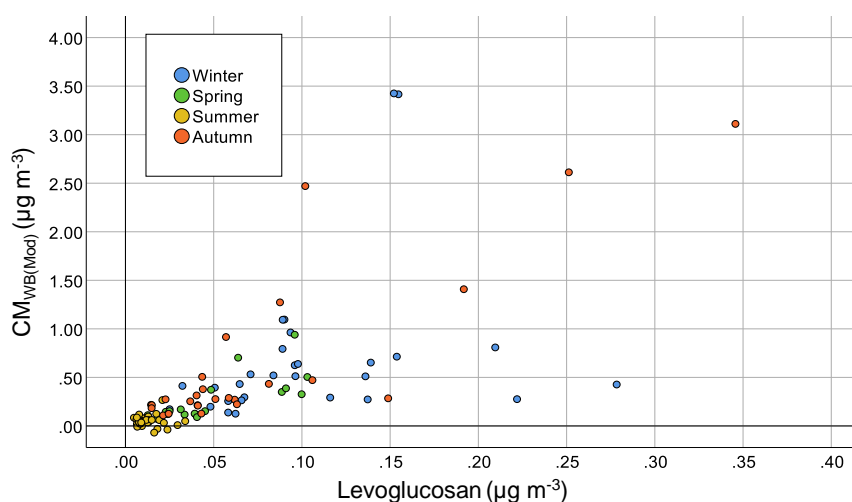


Fig. 3. Scatter plot displaying the relation between levoglucosan and $CM_{WB(Mod)}$. $N = 106$; $R^2 = 0.46$.

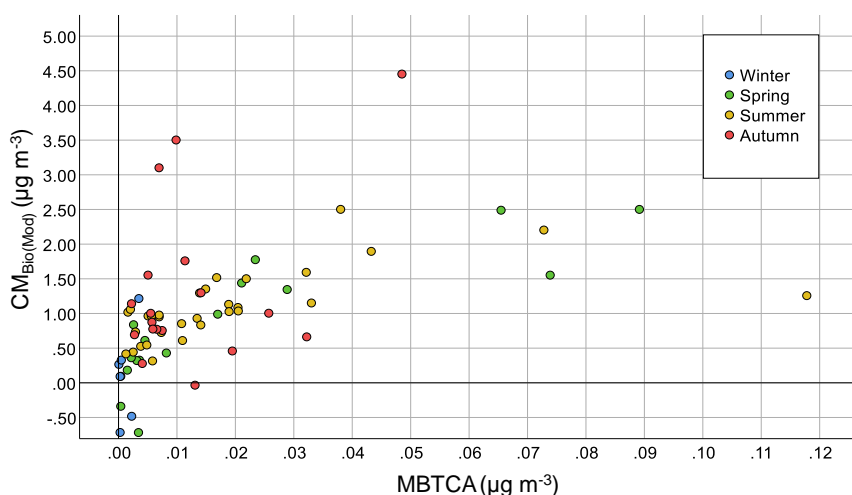


Fig. 4. Scatter plot displaying the relation between MBTCA and $CM_{Bio(Mod)}$. $N = 81$; $R^2 = 0.27$.

(i.e., mainly isoprene) should be included in future studies when investigating the residual carbon of the aethalometer model.

All three sources displayed positive correlation between their calculated carbon mass concentrations and air masses from the southeastern sector ($R^2_{CMFF(Mod)} = 0.37$, $p < 0.01$; $R^2_{CMWB(Mod)} = 0.38$, $p < 0.01$; $R^2_{CMBio(Mod)} = 0.14$, $p < 0.01$). On the other hand, air masses from the northwestern sector (i.e., the North sea and Atlantic ocean) seemed to have a negative effect on the mass concentration from the three sources ($R^2_{CMFF(Mod)} = 0.17$, $p < 0.01$; $R^2_{CMWB(Mod)} = 0.12$, $p < 0.01$; $R^2_{CMBio(Mod)} = 0.07$, $p < 0.01$).

Relationship between MBTCA and Aethalometer Model Parameters

Surprisingly we found that the MBTCA concentration show a significant correlation with the aethalometer model light absorption for fossil fuel carbon ($b_{absFF(950nm)}$) (Fig. 5, $R^2 = 0.20$, $p < 0.01$). Although the whole year correlation is low, there is a clear covariance during spring ($R^2 = 0.47$, $p < 0.01$) and fall ($R^2 = 0.58$, $p < 0.01$). During the winter, the MBTCA

concentrations are greatly suppressed and hence are unable to show any relationship to $b_{absFF(950nm)}$. Similar correlation is lacking when studying the whole-year relationship between MBTCA and $b_{absWB(370nm)}$ ($R^2 = 0.01$, $p = 0.39$). Further, no significant relationships could be established between the other biogenic tracers and $b_{absFF(950nm)}$. The Pearson correlation coefficient between MBTCA and the absorption coefficients derived from the seven wavelengths of the aethalometer show an increasing trend with higher wavelengths, and thus we find the highest correlation coefficient for 950 nm (0.23, Fig. S3). This finding leads to several speculations. To the authors' knowledge, no studies exist on the investigation on the light absorption properties of the MBTCA molecule, hence one option is that MBTCA itself display light absorptive properties in the infrared region of the UV-IR spectra. Another option might be co-transport of biogenic aerosols containing MBTCA and aerosols with high absorption in 950 nm (i.e., soot) from similar geographical regions. As mentioned above, air masses from the southeastern sector are more polluted than air masses from other regions, this has been seen in previous publications from the Vavihill

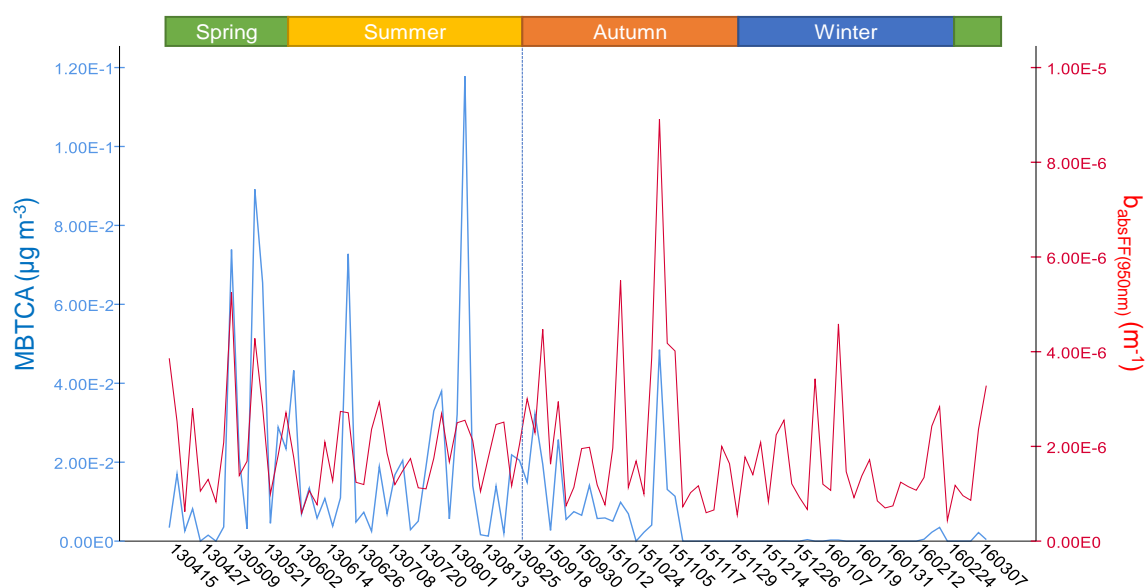


Fig. 5. Time series of MBTCA and $b_{\text{absFF}(950\text{nm})}$. Upper colored bar displays the different seasons. The dotted line in the transition between summer and autumn displays the transition between the measurement period of 2013 and 2015–2016. $N_{\text{MBTCA}} = 81$, $N_{b_{\text{absFF}(950\text{nm})}} = 106$; $R^2 = 0.20$.

measurement station (Kristensson *et al.*, 2008; Martinsson *et al.*, 2017b). Air masses from the southeastern sector of the Vavihill measurement station may originate from central Europe (eastern Germany, Czech Republic, Hungary, Slovakia and Poland) as well as major parts of eastern Europe (Ukraine, Belarus, Lithuania and Russia). We find large forests in parts of this sector, especially in Belarus, northern Ukraine northwestern Poland and Slovakia. With these facts in mind it is very possible that the co-variation between MBTCA and $b_{\text{absFF}(950\text{nm})}$ is explained by a co-transport rather than measurement detection of MBTCA in $b_{\text{absFF}(950\text{nm})}$. However, this speculation is contradicted by the low abundance of air masses from the southeastern sector which is only 13% for the whole measurement period. As stated above the correlation between $b_{\text{absFF}(950\text{nm})}$ and MBTCA was the highest during spring and fall, however the southeasterly air masses only occurred around 17% of the time during these seasons.

We investigated the light absorption of MBTCA through spectrophotometric analysis, the results are presented in Fig. 6. Regardless of the concentration, MBTCA showed distinct absorption peaks around 200–250 nm and 350–450 nm. In the wavelength region of interest for this discussion (> 800 nm) there is a small increase in absorption. Unfortunately, due to the upper wavelength range of the instrument (850 nm) we are not able to study the absorption up to 950 nm. Despite the absorption increase above 800 nm it is unlikely that this increase would explain any covariation between MBTCA and $b_{\text{abs}(950\text{nm})}$ for three reasons. First, the MBTCA mass used in the liquid solutions for the spectrophotometric analysis exceeds the ambient aerosol mass concentrations during summer (mean of 19 ng m^{-3}) by 8–10 orders of magnitude. As an example, a MBTCA solution of 10 mmol L^{-1} corresponds to approximately 0.05 g MBTCA in 25 mL ultrapure water. Hence it is likely that a realistic ambient aerosol MBTCA

concentration used in spectrophotometric analysis would give results below the detection limit. Second, brown carbon (BrC), a term for organic chemical compounds with enhanced light absorption in the UV-blue range that are produced in large quantities through biomass combustion, but can also be found in humic-like substances (HULIS) derived from biogenic oxidation products, is detectable in the aethalometer (Sandradewi *et al.*, 2008b; Laskin *et al.*, 2015) but has a light absorption per mass ($\alpha \rho^{-1}$) that is 4–5 orders of magnitude higher than the results from the spectrophotometric analysis (Chen and Bond, 2010). Third, if the experimental concentrations used in the spectrophotometric analysis would have had a significant impact in the aethalometer data, the 370 nm channel, i.e., $b_{\text{absWB}(370\text{nm})}$, would also have correlated with MBTCA due to the absorption peak observed around 400 nm (Fig. 6).

Liu *et al.* (2016) presented a spectrum for mass absorption coefficients (MAC) for the MBTCA precursor α -pinene. It was evident that the MAC value for α -pinene in 370 nm is negligible while it is elevated at wavelengths above 600 nm. Hence, it is possible that the observed correlation between MBTCA and $b_{\text{absFF}(950\text{nm})}$ is explained by presence of the weak IR absorber, and MBTCA precursor, α -pinene. Another option is that MBTCA are formed or co-emitted together with BC, originating from fossil fuel or biomass combustion. However, this option is highly doubtful and emission of MBTCA from fossil fuel combustion has to the author's knowledge never been proved or seen earlier. Although, it should be noted that both MBTCA and $b_{\text{absFF}(950\text{nm})}$ show increasing trends with a higher fraction of southeasterly air masses ($R^2 = 0.09$, $p = 0.03$ and $R^2 = 0.38$, $p < 0.01$ respectively), a geographic sector that has been shown to contribute with anthropogenic air pollutants (Kristensson *et al.*, 2008; Martinsson *et al.*, 2017b). The three remaining air mass sectors (NE, NW, SW) contribute with declining

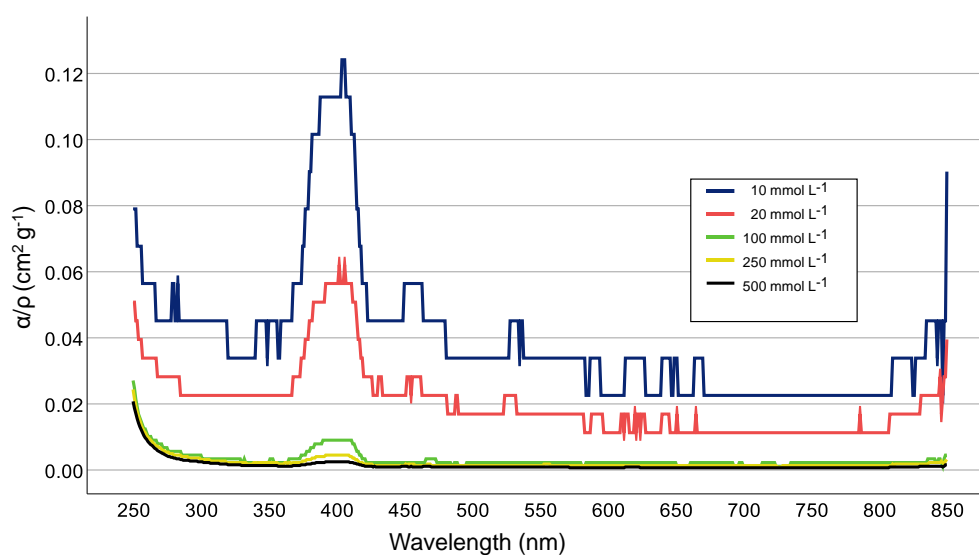


Fig. 6. Absorption per mass (α/p) for MBTCA. The wavelength section between 200–249 nm has been removed due to very high α/p values (> 6).

concentrations of MBTCA and $b_{\text{absFF}(950\text{nm})}$. An in depth investigation of the causes of this finding goes beyond the scope of this paper, however the suspicion from Martinsson *et al.* (2017b) that biogenic carbon might interfere and possibly obstruct the CM_{FF} quantification in the aethalometer model is still unclear and demands further investigation. However, in this study the MBTCA concentrations was very low and in many cases below detection limit during winter, which is the period used for deriving the C parameters in the aethalometer model. Hence, in this study the C parameters should be spared the interference of the possible IR absorbing MBTCA molecule.

CONCLUSIONS

In this study, we demonstrated that four common biogenic tracers showed positive correlation with the aethalometer model residual carbon, apportioned as biogenic carbon, CM_{Bio} . We also illustrated the need and performance to modify and optimize the C parameters, in this case the C_1 parameter. It should be noted that such a modification demands a thorough comparison between the aethalometer model output parameters and a tracer-based source apportionment that includes radiocarbon, levoglucosan and biogenic tracer measurement. In this study we used radiocarbon and levoglucosan source apportionment data generated from a previous study conducted at the same measurement station. To conclude, several years of measurements may be needed in order to establish stable C parameters for a particular measurement station, an aethalometer instrument and a thermo-optical instrument.

Surprisingly, we also found that MBTCA displayed a positive correlation with the derived absorption coefficients from fossil fuel carbonaceous aerosol, stressing the suspicion that biogenic aerosol might be falsely apportioned to this fraction. Hence, future studies should be directed towards experimental investigations with the aim of studying the light absorption properties of artificially produced biogenic

secondary organic aerosol. The experimental investigation should be parallel to further ambient aerosol studies utilizing high time resolved instrumentation such as the aerosol mass spectrometer as a complement to wet chemistry filter analysis.

ACKNOWLEDGEMENTS

This work was supported by the Swedish Research Council FORMAS (project 2011-743). An acknowledgement is given to Dr. Daniel Molins Delgado who supported with the spectrophotometric instrumentation.

SUPPLEMENTARY MATERIAL

Supplementary data associated with this article can be found in the online version at <https://doi.org/10.4209/aaqr.2020.01.0035>

REFERENCES

- Andersson-Sköld, Y. and Simpson, D. (2001). Secondary organic aerosol formation in northern Europe: A model study. *J. Geophys. Res.* 106: 7357–7374. <https://doi.org/10.1029/2000JD900656>
- Barregard, L., Sällsten, G., Gustafson, P., Johansson, L., Andersson, L. and Stigendal, L. (2006). Experimental exposure to wood smoke particles in healthy humans: Effects on markers of inflammation and coagulation. *Epidemiology* 17: S160–S161. <https://doi.org/10.1080/08958370600685798>
- Bauer, H., Claeys, M., Vermeylen, R., Schueller, E., Weinke, G., Berger, A. and Puxbaum, H. (2008). Arabitol and mannitol as tracers for the quantification of airborne fungal spores. *Atmos. Environ.* 42: 588–593. <https://doi.org/10.1016/j.atmosenv.2007.10.013>
- Bolling, A.K., Pagels, J., Yttri, K.E., Barregard, L., Sällsten, G., Schwarze, P.E. and Boman, C. (2009). Health effects

- of residential wood smoke particles: The importance of combustion conditions and physicochemical particle properties. *Part. Fibre Toxicol.* 6: 29. <https://doi.org/10.1186/1743-8977-6-29>
- Bond, T.C. and Bergstrom, R.W. (2006). Light absorption by carbonaceous particles: An investigative review. *Aerosol Sci. Technol.* 40: 27–67. <https://doi.org/10.1080/02786820500421521>
- Bond, T.C., Doherty, S.J., Fahey, D.W., Forster, P.M., Berntsen, T., DeAngelo, B.J., Flanner, M.G., Ghan, S., Karcher, B., Koch, D., Kinne, S., Kondo, Y., Quinn, P.K., Sarofim, M.C., Schultz, M.G., Schulz, M., Venkataraman, C., Zhang, H., Zhang, S., Bellouin, N., Guttikunda, S.K., Hopke, P.K., Jacobson, M.Z., Kaiser, J.W., Klimont, Z., Lohmann, U., Schwarz, J.P., Shindell, D., Storelvmo, T., Warren, S.G. and Zender, C.S. (2013). Bounding the role of black carbon in the climate system: A scientific assessment. *J. Geophys. Res.* 118: 5380–5552. <https://doi.org/10.1002/jgrd.50171>
- Burshtein, N., Lang-Yona, N. and Rudich, Y. (2011). Ergosterol, arabinol and mannitol as tracers for biogenic aerosols in the eastern Mediterranean. *Atmos. Chem. Phys.* 11: 829–839. <https://doi.org/10.5194/acp-11-829-2011>
- Caseiro, A., Marr, I.L., Claeys, M., Kasper-Giebl, A., Puxbaum, H. and Pio, C.A. (2007). Determination of Saccharides in atmospheric aerosol using anion-exchange high-performance liquid chromatography and pulsed-amperometric detection. *J. Chromatogr. A* 1171: 37–45. <https://doi.org/10.1016/j.chroma.2007.09.038>
- Cavalli, F., Alastuey, A., Areskoug, H., Ceburnis, D., Cech, J., Genberg, J., Harrison, R.M., Jaffrezo, J.L., Kiss, G., Laj, P., Mihalopoulos, N., Perez, N., Quincey, P., Schwarz, J., Sellegri, K., Spindler, G., Swietlicki, E., Theodosi, C., Yttri, K.E., Aas, W. and Putaud, J.P. (2016). A European aerosol phenomenology -4: Harmonized concentrations of carbonaceous aerosol at 10 regional background sites across Europe. *Atmos. Environ.* 144: 133–145. <https://doi.org/10.1016/j.atmosenv.2016.07.050>
- Cavalli, F., Viana, M., Yttri, K.E., Genberg, J. and Putaud, J.P. (2010). Toward a standardised thermal-optical protocol for measuring atmospheric organic and elemental carbon: The EUSAAR protocol. *Atmos. Meas. Tech.* 3: 79–89. <https://doi.org/10.5194/amt-3-79-2010>
- Chen, Y. and Bond, T.C. (2010). Light Absorption by Organic Carbon from Wood Combustion. *Atmos. Chem. Phys.* 10: 1773–1787. <https://doi.org/10.5194/acp-10-1773-2010>
- Cowie, G.L. and Hedges, J.I. (1984). Carbohydrate sources in a coastal marine-environment. *Geochim. Cosmochim. Acta* 48: 2075–2087.
- Donahue, N.M., Ortega, I.K., Chuang, W., Riipinen, I., Riccobono, F., Schobesberger, S., Dommen, J., Baltensperger, U., Kulmala, M., Worsnop, D.R. and Vehkamäki, H. (2013). How do organic vapors contribute to new-particle formation? *Faraday Discuss.* 165: 91–104. <https://doi.org/10.1039/C3FD00046J>
- Draxier, R.R. and Hess, G.D. (1998). An overview of the HYSPLIT_4 modelling system for trajectories, dispersion, and deposition. *Aust. Meteorol. Mag.* 47: 295–308.
- Drinovec, L., Mocnik, G., Zotter, P., Prevot, A.S.H., Ruckstuhl, C., Coz, E., Rupakheti, M., Sciare, J., Müller, T., Wiedensohler, A. and Hansen, A.D.A. (2015). The "dual-spot" Aethalometer: An improved measurement of aerosol black carbon with real-time loading compensation. *Atmos. Meas. Tech.* 8: 1965–1979. <https://doi.org/10.5194/amt-8-1965-2015>
- Fu, P.Q., Kawamura, K., Chen, J. and Barrie, L.A. (2009). Isoprene, monoterpene, and sesquiterpene oxidation products in the high Arctic aerosols during late winter to early summer. *Environ. Sci. Technol.* 43: 4022–4028. <https://doi.org/10.1021/es803669a>
- Fuzzi, S., Baltensperger, U., Carslaw, K., Decesari, S., van der Gon, H.D., Facchini, M.C., Fowler, D., Koren, I., Langford, B., Lohmann, U., Nemitz, E., Pandis, S., Riipinen, I., Rudich, Y., Schaap, M., Slowik, J.G., Spracklen, D.V., Vignati, E., Wild, M., Williams, M. and Gilardoni, S. (2015). Particulate matter, air quality and climate: Lessons learned and future needs. *Atmos. Chem. Phys.* 15: 8217–8299. <https://doi.org/10.5194/acp-15-8217-2015>
- Gabric, A., Gregg, W., Najjar, R., Erickson, D. and Matrai, P. (2001). Modeling the biochemical cycle of dimethylsulfide in the upper ocean: A review. *Chemosphere - Global Change Sci.* 3: 377–392. [https://doi.org/10.1016/S1465-9972\(01\)00018-6](https://doi.org/10.1016/S1465-9972(01)00018-6)
- Gao, S., Surratt, J.D., Knipping, E.M., Edgerton, E.S., Shahgholi, M. and Seinfeld, J.H. (2006). Characterization of polar organic components in fine aerosols in the southeastern United States: Identity, origin, and evolution. *J. Geophys. Res.* 111: D14314. <https://doi.org/10.1029/2005JD006601>
- Gelencser, A., May, B., Simpson, D., Sanchez-Ochoa, A., Kasper-Giebl, A., Puxbaum, H., Caseiro, A., Pio, C. and Legrand, M. (2007). Source apportionment of PM_{2.5} organic aerosol over Europe: Primary/secondary, natural/anthropogenic, and fossil/biogenic origin. *J. Geophys. Res.* 112: D23S04. <https://doi.org/10.1029/2006JD008094>
- Genberg, J., Hyder, M., Stenström, K., Bergström, R., Simpson, D., Fors, E.O., Jönsson, J.A. and Swietlicki, E. (2011). Source apportionment of carbonaceous aerosol in southern Sweden. *Atmos. Chem. Phys.* 11: 11387–11400. <https://doi.org/10.5194/acp-11-11387-2011>
- Glasius, M. and Goldstein, A.H. (2016). Recent discoveries and future challenges in atmospheric organic chemistry. *Environ. Sci. Technol.* 50: 2754–2764. <https://doi.org/10.1021/acs.est.5b05105>
- Guenther, A.B., Zimmerman, P.R., Harley, P.C., Monson, R.K. and Fall, R. (1993). Isoprene and monoterpene emission rate variability: Model evaluations and sensitivity analyses. *J. Geophys. Res.* 98: 12609–12617. <https://doi.org/10.1029/93JD00527>
- Guenther, A., Hewitt, C.N., Erickson, D., Fall, R., Geron, C., Graedel, T., Harley, P., Klinger, L., Lerdau, M., McKay, W.A., Pierce, T., Scholes, B., Steinbrecher, R., Tallamraju, R., Taylor, J. and Zimmerman, P. (1995). A global-model of natural volatile organic-compound emissions. *J. Geophys. Res.* 100: 8873–8892. <https://doi.org/10.1029/94JD02950>

- Guenther, A.B., Jiang, X., Heald, C.L., Sakulyanontvittaya, T., Duhl, T., Emmons, L.K. and Wang, X. (2012). The Model of Emissions of Gases and Aerosols from Nature version 2.1 (MEGAN2.1): An extended and updated framework for modeling biogenic emissions. *Geosci. Model Dev.* 5: 1471–1492. <https://doi.org/10.5194/gmd-5-1471-2012>
- Hakola, H., Hellen, H., Hemmila, M., Rinne, J. and Kulmala, M. (2012). In situ measurements of volatile organic compounds in a boreal forest. *Atmos. Chem. Phys.* 12: 11665–11678. <https://doi.org/10.5194/acp-12-11665-2012>
- Hakola, H., Tarvainen, V., Laurila, T., Hiltunen, V., Hellen, H. and Keronen, P. (2003). Seasonal variation of VOC concentrations above a boreal coniferous forest. *Atmos. Environ.* 37: 1623–1634. [https://doi.org/10.1016/S1352-2310\(03\)00014-1](https://doi.org/10.1016/S1352-2310(03)00014-1)
- Henry, K.M. and Donahue, N.M. (2012). Photochemical aging of α -pinene secondary organic aerosol: Effects of OH radical sources and photolysis. *J. Phys. Chem. A* 116: 5932–5940. <https://doi.org/10.1021/jp210288s>
- IPCC (2013). Summary for Policymakers. In *Climate Change 2013: The Physical Science Basis. Contribution of Working Group I to the Fifth Assessment Report of the Intergovernmental Panel on Climate Change*, Stocker, T.F., Qin, D., Plattner, G.K., Tignor, M., Allen, S.K., Boschung, J., Nauels, A., Xia, Y., Bex, V. and Midgley, P.M. (Eds.), Cambridge University Press, Cambridge, United Kingdom and New York, NY, USA.
- Janssen, N.A.H., Hoek, G., Simic-Lawson, M., Fischer, P., van Bree, L., ten Brink, H., Keuken, M., Atkinson, R.W., Anderson, H.R., Brunekreef, B. and Cassee, F.R. (2011). Black carbon as an additional indicator of the adverse health effects of airborne particles compared with PM₁₀ and PM_{2.5}. *Environ. Health Perspect.* 119: 1691–1699. <https://doi.org/10.1289/ehp.1003369>
- Jaoui, M. and Kamens, R.M. (2002). Mass balance of gaseous and particulate products analysis from α -pinene/NO_x/air in the presence of natural sunlight. *J. Geophys. Res.* 106: 12541–12558. <https://doi.org/10.1029/2001JD900005>
- Kanakidou, M., Seinfeld, J.H., Pandis, S.N., Barnes, I., Dentener, F.J., Facchini, M.C., Van Dingenen, R., Ervens, B., Nenes, A., Nielsen, C.J., Swietlicki, E., Putaud, J.P., Balkanski, Y., Fuzzi, S., Horth, J., Moortgat, G.K., Winterhalter, R., Myhre, C.E.L., Tsigaridis, K., Vignati, E., Stephanou, E.G. and Wilson, J. (2005). Organic aerosol and global climate modelling: A review. *Atmos. Chem. Phys.* 5: 1053–1123. <https://doi.org/10.5194/acp-5-1053-2005>
- Kostenidou, E., Karnezi, E., Kolodziejczyk, A., Szmigielski, R. and Pandis, S.N. (2018). Physical and chemical properties of 3-methyl-1,2,3-butanetricarboxylic acid (MBTCA) aerosol. *Environ. Sci. Technol.* 52: 1150–1155. <https://doi.org/10.1021/acs.est.7b04348>
- Kourtchev, I., Ruuskanen, T.M., Keronen, P., Sogacheva, L., Dal Maso, M., Reissell, A., Chi, X., Vermeylen, R., Kulmala, M., Maenhaut, W. and Claeys, M. (2008a). Determination of isoprene and α - β -pinene oxidation products in boreal forest aerosols from Hyytiälä, Finland: diel variations and possible link with particle formation events. *Plant Biol.* 10: 138–149. <https://doi.org/10.1055/s-2007-964945>
- Kourtchev, I., Warnke, J., Maenhaut, W., Hoffmann, T. and Claeys, M. (2008b). Polar organic marker compounds in PM_{2.5} aerosol from a mixed forest site in western Germany. *Chemosphere* 73: 1308–1314. <https://doi.org/10.1016/j.chemosphere.2008.07.011>
- Kourtchev, I., Copolovici, L., Claeys, M. and Maenhaut, W. (2009). Characterization of atmospheric aerosols at a forested site in central Europe. *Environ. Sci. Technol.* 43: 4665–4671. <https://doi.org/10.1021/es803055w>
- Kristensen, K. and Glasius, M. (2011). Organosulfates and oxidation products from biogenic hydrocarbons in fine aerosols from a forest in North West Europe during spring. *Atmos. Environ.* 45: 4546–4556. <https://doi.org/10.1016/j.atmosenv.2011.05.063>
- Kristensson, A., Dal Maso, M., Swietlicki, E., Hussein, T., Zhou, J., Kerminen, V.M. and Kulmala, M. (2008). Characterization of New particle formation events at a background site in southern Sweden: Relation to air mass history. *Tellus B* 60: 330–344. <https://doi.org/10.1111/j.1600-0889.2008.00345.x>
- Kubatova, A., Vermeylen, R., Claeys, M., Cafmeyer, J., Maenhaut, W., Roberts, G. and Artaxo, P. (2000). Carbonaceous aerosol characterization in the Amazon basin, Brazil: Novel dicarboxylic acids and related compounds. *Atmos. Environ.* 34: 5037–5051. [https://doi.org/10.1016/S1352-2310\(00\)00320-4](https://doi.org/10.1016/S1352-2310(00)00320-4)
- Kubatova, A., Vermeylen, R., Claeys, M., Cafmeyer, J. and Maenhaut, W. (2002). Organic compounds in urban aerosols from Gent, Belgium: Characterization, sources, and seasonal differences. *J. Geophys. Res.* 107: 8343. <https://doi.org/10.1029/2001JD000556>
- Laothawornkitkul, J., Taylor, J.E., Paul, N.D. and Hewitt, C.N. (2009). Biogenic volatile organic compounds in the Earth system. *New Phytol.* 183: 27–51. <https://doi.org/10.1111/j.1469-8137.2009.02859.x>
- Larsen, B.R., Di Bella, D., Glasius, M., Winterhalter, R., Jensen, N.R. and Hjorth, J. (2001). Gas-phase ozone oxidation of monoterpenes: Gaseous and particulate products. *J. Atmos. Chem.* 38: 231–276. <https://doi.org/10.1023/A:1006487530903>
- Laskin, A., Laskin, J. and Nizkorodov, S.A. (2015). Chemistry of atmospheric brown carbon. *Chem. Rev.* 115: 4335–4382. <https://doi.org/10.1021/cr5006167>
- Laskin, J., Laskin, A., Nizkorodov, S.A., Roach, P., Eckert, P., Gilles, M.K., Wang, B.B., Lee, H.J. and Hu, Q.C. (2014). Molecular selectivity of brown carbon chromophores. *Environ. Sci. Technol.* 48: 12047–12055. <https://doi.org/10.1021/acs.est.6b03024>
- Lee, A., Goldstein, A.H., Keywood, M.D., Gao, S., Varutbangkul, V., Bahreini, R., Ng, N.L., Flagan, R.C. and Seinfeld, J.H. (2006). Gas-phase products and secondary aerosol yields from the ozonolysis of ten different terpenes. *J. Geophys. Res.* 111: D07302. <https://doi.org/10.1029/2005JD006437>
- Lewandowski, M., Jaoui, M., Kleindienst, T.E., Offenberg,

- J.H. and Edney, E.O. (2007). Composition of PM_{2.5} during the summer of 2003 in Research Triangle Park, North Carolina. *Atmos. Environ.* 41: 4073–4083. <https://doi.org/10.1016/j.atmosenv.2007.01.012>
- Lioussé, C., Penner, J.E., Chuang, C., Walton, J.J., Eddleman, H. and Cachier, H. (1996). A global three-dimensional model study of carbonaceous aerosols. *J. Geophys. Res.* 101: 19411–19432. <https://doi.org/10.1029/95JD03426>
- Liu, J.M., Lin, P., Laskin, A., Laskin, J., Kathmann, S.M., Wise, M., Caylor, R., Imholt, F., Selimovic, V. and Shilling, J.E. (2016). Optical properties and aging of light-absorbing secondary organic aerosol. *Atmos. Chem. Phys.* 16: 12815–12827. <https://doi.org/10.5194/acp-16-12815-2016>
- Maenhaut, W., Chi, X.G., Wang, W., Cafmeyer, J., Yasmeen, F., Vermeylen, R., Szmigielska, K., Janssens, I.A. and Claeys, M. (2017). Contribution from selected organic species to PM_{2.5} aerosol during a summer field campaign at K-Puszta, Hungary. *Atmosphere* 8: 221. <https://doi.org/10.3390/atmos8110221>
- Manninen, H.E., Back, J., Sihto-Nissila, S.L., Huffman, J.A., Pessi, A.M., Hiltunen, V., Aalto, P.P., Hidalgo, P.J., Hari, P., Saarto, A., Kulmala, M. and Petaja, T. (2014). Patterns in airborne pollen and other primary biological aerosol particles (PBAP), and their contribution to aerosol mass and number in a boreal forest. *Boreal Environ. Res.* 19: 383–405.
- Martinsson, J., Andersson, A., Sporre, M.K., Friberg, J., Kristensson, A., Swietlicki, E., Olsson, P.A. and Stenström, K.E. (2017a). Evaluation of $\delta^{13}\text{C}$ in carbonaceous aerosol source apportionment at a rural measurement site. *Aerosol Air Qual Res* 17: 2081–2094. <https://doi.org/10.4209/aaqr.2016.09.0392>
- Martinsson, J., Azeem, H.A., Sporre, M.K., Bergstrom, R., Ahlberg, E., Östrom, E., Kristensson, A., Swietlicki, E. and Stenström, K.E. (2017b). Carbonaceous aerosol source apportionment using the Aethalometer model – evaluation by radiocarbon and levoglucosan analysis at a rural background site in southern Sweden. *Atmos. Chem. Phys.* 17: 4265–4281. <https://doi.org/10.5194/acp-17-4265-2017>
- Martinsson, J., Monteil, G., Sporre, M.K., Hansen, A.M.K., Kristensson, A., Stenström, K.E., Swietlicki, E. and Glasius, M. (2017c). Exploring sources of biogenic secondary organic aerosol compounds using chemical analysis and the FLEXPART model. *Atmos. Chem. Phys.* 17: 11025–11040. <https://doi.org/10.5194/acp-17-11025-2017>
- Monson, R.K., Jones, R.T., Rosenstiel, T.N. and Schnitzler, J.P. (2013). Why only some plants emit isoprene. *Plant Cell Environ.* 36: 503–516. <https://doi.org/10.1111/pce.12015>
- Müller, L., Reinnig, M.C., Naumann, K.H., Saathoff, H., Mentel, T.F., Donahue, N.M. and Hoffmann, T. (2012). Formation of 3-methyl-1,2,3-butanetricarboxylic acid via gas phase oxidation of pinonic acid – a mass spectrometric study of SOA aging. *Atmos. Chem. Phys.* 12: 1483–1496. <https://doi.org/10.5194/acp-12-1483-2012>
- Naeher, L.P., Brauer, M., Lipsett, M., Zelikoff, J.T., Simpson, C.D., Koenig, J.Q. and Smith, K.R. (2007). Woodsmoke health effects: A review. *Inhalation Toxicol.* 19: 67–106. <https://doi.org/10.1080/08958370600985875>
- Nakayama, T., Matsumi, Y., Sato, K., Imamura, T., Yamazaki, A. and Uchiyama, A. (2010). Laboratory studies on optical properties of secondary organic aerosols generated during the photooxidation of toluene and the ozonolysis of α -pinene. *J. Geophys. Res.* 115: D24204. <https://doi.org/10.1029/2010JD014387>
- Penuelas, J. and Llusia, J. (2003). BVOCs: plant defense against climate warming? *Trends Plant Sci.* 8: 105–109. [https://doi.org/10.1016/S1360-1385\(03\)00008-6](https://doi.org/10.1016/S1360-1385(03)00008-6)
- Pietrogrande, M.C., Bacco, D., Visentin, M., Ferrari, S. and Poluzzi, V. (2014). Polar organic marker compounds in atmospheric aerosol in the Po Valley during the Supersito campaigns – Part 1: Low molecular weight carboxylic acids in cold seasons. *Atmos. Environ.* 86: 164–175. <https://doi.org/10.1016/j.atmosenv.2013.12.022>
- Putaud, J.P., Van Dingenen, R., Alastuey, A., Bauer, H., Birmili, W., Cyrys, J., Flentje, H., Fuzzi, S., Gehrig, R., Hansson, H.C., Harrison, R.M., Herrmann, H., Hitzenberger, R., Hüglin, C., Jones, A.M., Kasper-Giebl, A., Kiss, G., Kousa, A., Kuhlbusch, T.A.J., Loschau, G., Maenhaut, W., Molnar, A., Moreno, T., Pekkanen, J., Perrino, C., Pitz, M., Puxbaum, H., Querol, X., Rodriguez, S., Salma, I., Schwarz, J., Smolik, J., Schneider, J., Spindler, G., ten Brink, H., Tursic, J., Viana, M., Wiedensohler, A. and Raes, F. (2010). A European aerosol phenomenology – 3: Physical and chemical characteristics of particulate matter from 60 rural, urban, and kerbside sites across Europe. *Atmos. Environ.* 44: 1308–1320. <https://doi.org/10.1016/j.atmosenv.2009.12.011>
- Räsänen, T., Ryppö, A. and Kellomäki, S. (2008). Effects of elevated CO₂ and temperature on monoterpene emission of Scots pine (*Pinus sylvestris* L.) *Atmos. Environ.* 42: 4160–4171. <https://doi.org/10.1016/j.atmosenv.2008.01.023>
- Sandradewi, J., Prevot, A.S.H., Szidat, S., Perron, N., Alfarra, M.R., Lanz, V.A., Weingartner, E. and Baltensperger, U. (2008a). Using aerosol light absorption measurements for the quantitative determination of wood burning and traffic emission contributions to particulate matter. *Environ. Sci. Technol.* 42: 3316–3323. <https://doi.org/10.1021/es702253m>
- Sandradewi, J., Prevot, A.S.H., Weingartner, E., Schmidhauser, R., Gysel, M. and Baltensperger, U. (2008b). A study of wood burning and traffic aerosols in an Alpine valley using a multi-wavelength Aethalometer. *Atmos. Environ.* 42: 101–112. <https://doi.org/10.1016/j.atmosenv.2007.09.034>
- Sehlstedt, M., Dove, R., Boman, C., Pagels, J., Swietlicki, E., Löndahl, J., Westerholm, R., Bosson, J., Barath, S., Behndig, A.F., Pourazar, J., Sandström, T., Mudway, I.S. and Blomberg, A. (2010). Antioxidant airway responses following experimental exposure to wood smoke in man. *Part. Fibre Toxicol.* 7: 21. <https://doi.org/10.1186/1743-8977-7-21>
- Sharkey, T.D., Wiberley, A.E. and Donohue, A.R. (2008). Isoprene emission from plants: Why and how. *Ann. Bot.*

- 101: 5–18. <https://doi.org/10.1093/aob/mcm240>
- Siljamo, P., Sofiev, M., Severova, E., Ranta, H., Kukkonen, J., Polevova, S., Kubin, E. and Minin, A. (2008). Sources, impact and exchange of early-spring birch pollen in the Moscow region and Finland. *Aerobiologia* 24: 211–230. <https://doi.org/10.1007/s10453-008-9100-8>
- Speranza, A., Calzoni, G.L. and Pacini, E. (1997). Occurrence of mono- or disaccharides and polysaccharide reserves in mature pollen grains. *Sex. Plant Reprod.* 10: 110–115. <https://doi.org/10.1007/s004970050076>
- Sporre, M.K., Blichner, S.M., Karset, I.H.H., Makkonen, R. and Berntsen, T.K. (2019). BVOC–aerosol–climate feedbacks investigated using NorESM. *Atmos. Chem. Phys.* 19: 4763–4782. <https://doi.org/10.5194/acp-19-4763-2019>
- Stein, A.F., Draxler, R.R., Rolph, G.D., Stunder, B.J.B., Cohen, M.D. and Ngan, F. (2015). NOAA's HYSPLIT atmospheric transport and dispersion modeling system. *Bull. Amer. Meteor. Soc.* 96: 2059–2077. <https://doi.org/10.1175/BAMS-D-14-00110.1>
- Steinke, M., Hodapp, B., Subhan, R., Bell, T.G. and Martin-Creuzburg, D. (2018). Flux of the biogenic volatiles isoprene and dimethyl sulfide from an oligotrophic lake. *Sci. Rep.* 8: 630. <https://doi.org/10.1038/s41598-017-18923-5>
- Szmigielski, R., Surratt, J.D., Gomez-Gonzalez, Y., Van der Veken, P., Kourtchev, I., Vermeylen, R., Blockhuys, F., Jaoui, M., Kleindienst, T.E., Lewandowski, M., Offenberg, J.H., Edney, E.O., Seinfeld, J.H., Maenhaut, W. and Claeys, M. (2007). 3-methyl-1,2,3-butanetricarboxylic acid: An atmospheric tracer for terpene secondary organic aerosol. *Geophys Res Lett* 34: L24811. <https://doi.org/10.1029/2007GL031338>
- Verma, S.K., Kawamura, K., Chen, J. and Fu, P.Q. (2018). Thirteen years of observations on primary sugars and sugar alcohols over remote Chichijima Island in the western North Pacific. *Atmos. Chem. Phys.* 18: 81–101. <https://doi.org/10.5194/acp-18-81-2018>
- Vogel, A.L., Åijälä, M., Corrigan, A.L., Junninen, H., Ehn, M., Petäjä, T., Worsnop, D.R., Kulmala, M., Russell, L.M., Williams, J. and Hoffmann, T. (2013). In situ submicron organic aerosol characterization at a boreal forest research station during HUMPPA-COPEC 2010 using soft and hard ionization mass spectrometry. *Atmos. Chem. Phys.* 13: 10933–10950. <https://doi.org/10.5194/acp-13-10933-2013>
- Weingartner, E., Saathoff, H., Schnaiter, M., Streit, N., Bitnar, B. and Baltensperger, U. (2003). Absorption of light by soot particles: determination of the absorption coefficient by means of aethalometers. *J. Aerosol Sci.* 34: 1445–1463. [https://doi.org/10.1016/S0021-8502\(03\)00359-8](https://doi.org/10.1016/S0021-8502(03)00359-8)
- Yasmeen, F., Szmigielski, R., Vermeylen, R., Gomez-Gonzalez, Y., Surratt, J.D., Chan, A.W.H., Seinfeld, J.H., Maenhaut, W. and Claeys, M. (2011). Mass spectrometric characterization of isomeric terpenic acids from the oxidation of α -pinene, β -pinene, d-limonene, and Δ^3 -carene in fine forest aerosol. *J. Mass Spectrom.* 46: 425–442. <https://doi.org/10.1002/jms.1911>
- Yli-Panula, E., Fekedulegn, D.B., Green, B.J. and Ranta, H. (2009). Analysis of airborne betula pollen in Finland; a 31-year perspective. *Int. J. Environ. Res. Public Health* 6: 1706–1723. <https://doi.org/10.3390/ijerph6061706>
- Yttri, K.E., Dye, C. and Kiss, G. (2007). Ambient aerosol concentrations of sugars and sugar-alcohols at four different sites in Norway. *Atmos. Chem. Phys.* 7: 4267–4279. <https://doi.org/10.5194/acp-7-4267-2007>
- Yttri, K.E., Simpson, D., Nojgaard, J.K., Kristensen, K., Genberg, J., Stenström, K., Swietlicki, E., Hillamo, R., Aurela, M., Bauer, H., Offenberg, J.H., Jaoui, M., Dye, C., Eckhardt, S., Burkhardt, J.F., Stohl, A. and Glasius, M. (2011). Source apportionment of the summer time carbonaceous aerosol at Nordic rural background sites. *Atmos. Chem. Phys.* 11: 13339–13357. <https://doi.org/10.5194/acp-11-13339-2011>
- Zhang, Y.Y., Muller, L., Winterhalter, R., Moortgat, G.K., Hoffmann, T. and Poschl, U. (2010). Seasonal cycle and temperature dependence of pinene oxidation products, dicarboxylic acids and nitrophenols in fine and coarse air particulate matter. *Atmos. Chem. Phys.* 10: 7859–7873. <https://doi.org/10.5194/acp-10-7859-2010>

Received for review, February 19, 2020

Revised, September 7, 2020

Accepted, September 8, 2020